

### Comparison of Different Models of Size-Dependent Thermodynamic Properties of Nanoparticles

**Abdulrhman Kh. Suliman**

*Physics Department. College of Science, Salahaddin University, Erbil, Iraq.*

*Received on: 8/1/2018;*

*Accepted on: 10/4/2018*

---

**Abstract:** Surface and thermodynamic properties, such as enthalpy, cohesive energy, surface energy and melting point, of different materials (Ag, Au, Sn and In) were calculated theoretically in this study by using the following two models: firstly, the lattice vibration-based model (*LVB*) of surface atoms and secondly, the surface-to-volume atom ratio (*SV/A*) model of the free surface nanoparticle material. In this work, the melting temperature and other thermodynamic properties of the modified model of the nanoparticles improved the calculated curve compared with that of the experimental data due to the effect of lattice volume. Results of the two models showed changes in all thermodynamic properties as nanoparticle size decreased. Moreover, compared with the experimental data, a good agreement was observed between the modified *LVB* model and the experimental data.

**Keywords:** Cohesive energy, Enthalpy, Melting point, Surface energy, Nanoparticles, Size effects.

**PACS:** 67.25.bd, 65.80.-g.

## Introduction

Thermodynamic properties of nanoscale materials are different from those of their corresponding bulk materials [1, 2]. Thus, understanding the surface and thermodynamic properties of nanoscale materials, for instance, crystals in carbon nanotubes and thin films of nanometer thickness, is vital because of their potential applications in microelectronics, nonlinear optics and solar energy [3-6]. The properties of bulk crystals depend on their structure. However, in addition to the structure, their size influences their properties, such as melting point, cohesive energy, entropy, thermal enthalpy, Debye temperature and surface energy, at the nanoscale [7]. Different models have been developed to explain and account for the thermodynamic properties of low-dimensional materials. These models include the liquid drop [8], bond-order-length-strength and latent heat models for size-dependent cohesive energy [9, 10]. These models also include surface area-

different and bond energy model [11], which is also used to predict the melting temperature of nanomaterials [12]. Moreover, a variety of theoretical calculation methods have been used to obtain surface energy of nanoparticles. These calculation methods include the broken-bond rule [13] and the modified embedded atom method [14]. Ouyang *et al.* (2006) and Jiang *et al.* (2010) experimentally measured the surface energies of nanocrystals and showed the dependence of nanoparticle properties on their sizes in metals and semiconductors [15, 7].

One of the important thermodynamic properties is cohesive energy, which determines a wide range of thermophysical properties, including melting point, solubility and surface energy. Surface energy is linear to cohesive energy, whereas cohesive energy is linear to melting point [16, 17]. Moreover, cohesive energy and melting point are parameters used for estimating metallic bond strength. A high

cohesive energy indicates high thermal stability of the materials [18]. Therefore, identifying the melting entropy and enthalpy is important to understand the stability of nanocrystals. Metal nanoparticles have properties intermediate between those of metals and non-metals. In this study, lattice vibration-based (*LVB*) and surface-to-volume atom ratio (*SVR*) models were applied to study the quantities that are dependent on the binding energies of nanocrystals. This investigation was performed to assess the proficiency of a model and showed results that agreed with the experimental data.

## Method of Calculation

The first physical model (*LVB*), is used in the present work to derive the size-dependent enthalpy and entropy based on the Mott's expression for the vibrational melting entropy  $S_{vib}$  [19]. The second model was *SVR*, which is a simple method that was developed in 2005 by Qi, W.H. [20], who emphasized that phase stability is sensitive to the surface-to-volume ratio of atoms.

### Lattice Vibration Based (*LVB*) Model

A physical model for size-dependent melting enthalpy  $H_m(r)$  is related to melting temperature  $T_m(r)$  and melting entropy  $S_m(r)$  which is a function of the specific heat difference between solid and liquid state [19, 21]; therefore,  $H_m(r)$  is equal to;

$$H_m(r) = T_m(r) \cdot S_m(r). \quad (1)$$

The modified model for melting temperature of nanoparticles  $T_m(r)$  due to the effect of lattice volume can be described by the following relation [22];

$$\frac{T_m(r)}{T_{mb}} = \left(\frac{V(r)}{Vb}\right)^{2/3} \exp\left(\frac{-2S_{mb}}{3R} \frac{1}{r_0-1}\right) \quad (2)$$

where  $T_{mb}$  is the bulk melting point,  $Vb$  is the bulk lattice volume,  $R$  is the ideal gas constant and  $r_0$  denotes the smallest size where there is no structural difference between the solid and the liquid states. At  $r_0$ , all atoms or molecules are located on the bulk surface.  $r_0$  can be extended for different dimensions  $D$ ; for nanoparticles  $D = 0$ , for nanowires  $D = 1$  and for thin films  $D = 2$ . For nanoparticles and nanowires,  $r$  is the radius and for thin films, it is the half thickness. The relationship between  $r_0$  and the first solid surface layer height  $h$  is shown as [8, 12, 16];

$$r_0 = (3-D) h. \quad (3)$$

For a spherical nanoparticle of  $r_0 = 3h$ , this value of  $h$  represents a length scale characteristic for crystallinity and is called critical radius. Its values for different elements used in this work are found in *Table 1* [23-25].

The size-dependent lattice volume  $V(r)$  is calculated as follows; the size-dependent lattice parameter  $a(r)$  is obtained from;  $a(r) = \frac{4}{\sqrt{3}} d_{mean}(r)$ , where  $d_{mean}(r)$  is the mean bond length of nanoparticles. Its value for bulk crystal  $d_{mean}(\infty)$  is constant for all elements listed in *Table 1*. The mean bond length for nanoparticles is given by the equation [22];

$$d_{mean}(r) = h - \Delta d_{mean}(r). \quad (4)$$

The change of mean bond length with size  $\Delta d_{mean}(r)$  is given by;

$$\Delta d_{mean}(r) = \Delta d_{mean}(r_0) \exp\left(\frac{-2S_{mb}}{3R} \frac{1}{r_0-1}\right) \quad (5)$$

where  $\Delta d_{mean}(r_0)$  is the maximum increase in the mean bond length  $d_{mean}(r)$ . Then, lattice volume  $V(r)$  of nanoparticles is calculated from the relation [2];  $V(r) = \frac{a(r)^3}{4}$ .

Melting entropy  $S_m(r)$  can be described by the following expression;

$$\frac{S_m(r)}{S_{mb}} = \left(1 - \frac{1}{r_0-1}\right) \quad (6)$$

where,  $S_{mb}$  is the bulk overall melting entropy. The model suggests that the size dependence of the melting entropy for nano-semiconductor nanoparticles is determined by the size dependence of the vibrational part of the melting entropy of nanocrystal  $S_{vib}$ , [7, 26]. The melting entropy for metallic and organic crystals is mainly vibrational in nature and  $S_{vib} = S_{mb}$ , [27]. From Eq. (2) and Eq. (6), size-dependent melting enthalpy  $H_m(r)$  from Eq. (1) is expressed as;

$$\frac{H_m(r)}{H_{mb}} = \left(\frac{V(r)}{Vb}\right)^{2/3} \left[\exp\left(\frac{2S_{vib}}{3R} \frac{1}{r_0-1}\right)\right] \cdot \left(1 - \frac{1}{r_0-1}\right) \quad (7)$$

where,  $H_{mb}$  is the bulk enthalpy and its value is given in *Table 1*, [7]. It is well known that the bulk melting point of most materials is proportional to their binding energy and their bulk cohesive energy  $E_{mb}$  is proportional to their binding energy. Transition entropy term for the

solid-vapor transition related to cohesive energy can be expressed as follows;

$$S_{mb} = E_{mb} / T_{mb}. \quad (8)$$

Bulk cohesive energy  $E_{mb}$  at  $T_{mb}$  being the bulk solid-vapor transition temperature, size-dependent cohesive energy  $E(r)$  is a linear function of melting point and is given to a good approximation as [28];

$$\frac{E(r)}{E_{mb}} = \frac{T_m(r)}{T_{mb}} \cdot \frac{S_m(r)}{S_{mb}}. \quad (9)$$

From Eq. (2) and Eq. (6), size-dependent cohesive energy of nanoparticles is expressed as [17, 30];

$$\frac{E(r)}{E_{mb}} = \left(\frac{V(r)}{V_b}\right)^{2/3} \left[ \exp\left(\frac{-2S_{vib}}{3R} \frac{1}{r_0-1}\right) \right] \cdot \left(1 - \frac{1}{r_0-1}\right). \quad (10)$$

The surface energy  $\gamma_{mb}$  is proportional to cohesive energy  $E_{mb}$  through the following relation;  $\gamma_{mb} = k E_{mb}$ , where  $k$  is constant and for size-dependent surface energy of nanoscale materials is [19, 31];  $\gamma(r) = k E(r)$ . By comparing the equations for  $(\gamma_{mb})$  and  $(\gamma(r))$ , the comprehensive equation of surface energy of nanoparticles will be;

$$\frac{\gamma(r)}{\gamma_{mb}} = \frac{E(r)}{E_{mb}}. \quad (11)$$

Therefore,

$$\frac{\gamma(r)}{\gamma_{mb}} = \left(\frac{V(r)}{V_b}\right)^{2/3} \left[ \exp\left(\frac{-2S_{vib}}{3R} \frac{1}{r_0-1}\right) \right] \cdot \left(1 - \frac{1}{r_0-1}\right). \quad (12)$$

### Surface to Volume Atom Ratio (SVA) Model

A very simple model has been developed and reported in ref. [20], showing the relation between the melting temperature of nanomaterial and bulk as;

$$\frac{T_m(r)}{T_{mb}} = \left(1 - \frac{N}{2n}\right) = \left(1 - \frac{2d}{rc}\right) \quad (13)$$

where  $N$  is the number of surface atoms of the structure and  $n$  is the total number of atoms. The method to find the rate  $N/2n$  for different types of nanomaterials has been introduced by (Qi, 2006) [11, 21]. According to the (SVA)

model [20],  $\frac{N}{n}$  is  $\frac{4d}{r_c}$ ,  $\frac{8d}{3L}$  and  $\frac{4d}{3W}$  for spherical nanoparticles, nanowires and nanofilms, respectively, where  $d$  is the atom diameter and  $r_c$  is the diameter of spherical nanoparticles. Here,  $L$  is the diameter of nanowires and  $W$  is the height of solid nanofilms [32].

The relation between crystal vibration entropy  $S_{vib}$  and melting point  $T_{mb}$  can be described as [32, 33];

$$S_{vib}(r) - S_{mb} = \frac{3R}{2} \ln \frac{T_m(r)}{T_{mb}} = \frac{3R}{2} \ln \left(1 - \frac{2d}{rc}\right) \quad (14)$$

where  $S_{mb}$  is the melting entropy of bulk solid crystal.  $H_m(r)$  is a linear function of melting point and is given as [9];

$$\frac{H_m(r)}{H_{mb}} = \left(\frac{S_m(r)}{S_{mb}}\right) \cdot \left(\frac{T_m(r)}{T_{mb}}\right). \quad (15)$$

Substituting Eq. (13) in Eq. (14), the size-dependent enthalpy for spherical nanoparticles is;

$$H_m(r) = T_{mb} \left(1 - \frac{2d}{rc}\right) \left[ S_{mb} + \frac{3R}{2} \ln \left(1 - \frac{2d}{rc}\right) \right] \quad (16)$$

$$H_m(r) = \left[ H_{mb} + \frac{3RT_{mb}}{2} \ln \left(1 - \frac{2d}{rc}\right) \right] \left(1 - \frac{2d}{rc}\right). \quad (17)$$

The linear relation between melting temperature and cohesive energy is [30];  $\frac{E(r)}{E_{mb}} = \frac{T_m(r)}{T_{mb}}$ ; therefore, size dependence cohesive energy  $E(r)$  expression in this model is [15];

$$E(r) = E_{mb} \left(1 - \frac{2d}{rc}\right). \quad (18)$$

The relationship between surface energy and cohesive energy is;

$$\frac{\gamma(D)}{\gamma_b} = \frac{E(r)}{E_{mb}}. \quad (19)$$

By using the value of cohesive energy from Eq. (18) in Eq. (19), size-dependent surface energy for nanoparticles is [19];

$$\gamma(r) = \gamma_b \left(1 - \frac{2d}{rc}\right). \quad (20)$$

TABLE 1. Thermodynamic and structure parameters for some solid elements concerned in this work, such as; bulk enthalpy  $H_{mb}$  (kJ/mol), bulk cohesive energy  $E_{mb}$  [kJ/mol], surface energy  $\gamma$  (J/m<sup>2</sup>), entropy  $S_{vib}$ (J/mole.K), mean bond length  $d_{mean}$  (nm), first surface layer height  $h$  (nm) [15, 23-25, 27, 34].

Substance	$h$ (nm)	$d_{mean}$ (nm)	$H_{mb}$ (kJ/mol)	$E_{mb}$ (kJ/mol)	$S_{vib}$ (J/mole.K)	$\gamma$ (J/m <sup>2</sup> )
Ag	0.3197	0.289	113	284	9.16	7.205
Au	0.3188	0.2884	125	368	9.38	1.28
In	0.3682	0.3291	328	284	7.59	1.205
Sn	0.281	0.376	720	303	9.22	0.68

## Results and Discussion

Fig. 1 illustrates a comparison between the predication of modified Eq. (2) (with and without the effect of lattice volume) with Eq. (13) and experimental  $T_m(r)$  data for metallic Au nanoparticles. The result of modified Eq. (2) is in agreement with the experimental data. Moreover, the bulk melting temperature of Au is 1337.58 K [25]. As shown in Fig. 1, the results of the modified  $LVB$  model, as predicated by Eq. (2) in calculating the melting temperature of nanoparticles due to the effect of lattice volume, were in good agreement with the range of the experimental data.

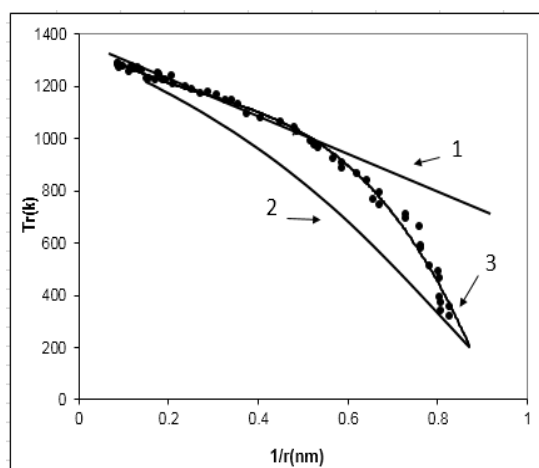


FIG. 1.  $T_m(r)$  function of the Au nanoparticle size, where number (1) on the figure represents the  $SVA$  model predication of Eq. (13), whereas (2) and (3) represent the  $LVB$  model and its modified predication of Eq. (2), respectively and the solid spheres ( $\bullet$ ) represent the experimental data obtained from Ref. [36].

The  $SVA$  model in the range ( $r < 10$  nm) gave higher results than the experimental results. The results of both models were different from the experimental data. Diwan and Kumar (2013) showed that the binding energy, cohesive energy and other thermodynamic properties, such as

entropy and enthalpy, approach their bulk value when the particle size is above 100 nm [17,35].

Figure 2 also shows that the cohesive energy of a nanoparticle approaches its bulk value when the nanoparticle size ( $r$ ) is far beyond the atomic size ( $r \gg d$ ).

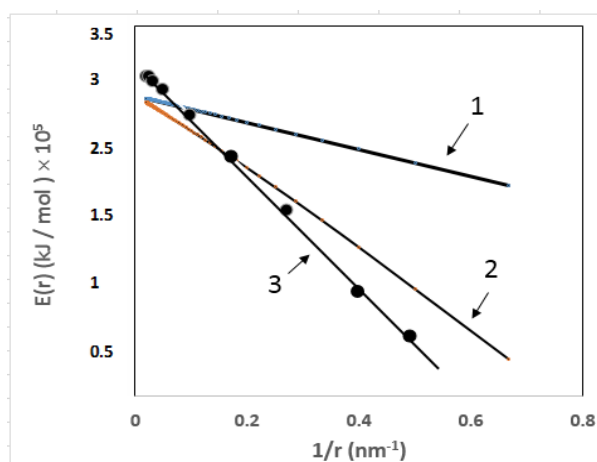


FIG. 2.  $E(r)$  function of Ag nanoparticle size, where number (1) represents the  $SVA$  model predication of Eq. (18), (2) represents the  $LVB$  model predication of Eq. (10), (3) is the modified predication of Eq (10) and the solid spheres ( $\bullet$ ) represent the experimental data obtained from Ref. [36].

entropy and enthalpy, approach their bulk value when the particle size is above 100 nm [17,35]. Figure 2 also shows that the cohesive energy of a nanoparticle approaches its bulk value when the nanoparticle size ( $r$ ) is far beyond the atomic size ( $r \gg d$ ).

According to our study, a clear matching can be obtained between both models and the experimental data when the nanoparticle size is larger than 20 nm. The cohesive energy of a nanocrystal is governed by nearest neighbor interactions. This phenomenon leads to a linear dependence of this cohesive energy on the inverse size (reciprocal radius) of nanoparticles [20, 23, 36].

For metals, the assumption of the nearest neighbor is good. However, for nonmetallic and semiconductor nanocrystals, this assumption is no longer valid, because covalency and ionicity play major roles in bonding and determining the cohesive energy [27].

The cohesive energy of nanoparticles may increase or decrease with the crystal size, depending on the surface atom bonds of nanoparticles. If the surface atoms have large dangling bonds, then the cohesive energy of the nanoparticle decreases with decreasing the crystal size. This result implies a decrease in the strength of metallic bond (i.e., easily break). In this case, the strength of the metallic bond for nanoparticles becomes weaker than those of the bulk metals [18, 27].

In Figs. 3–5, we present a comparison between the *LVB* model predication of Eq. (7) and the modified predication of Eq. (7), as well as between the *SVA* model predication of Eq. (17)

and the experimental results of  $H_{mb}(r)$  for Ag, In and Sn nanoparticles obtained from References [29, 37]. The results of the modified *LVB* model were in good agreement with the experimental data for In, Sn and Ag nanoparticles. For Sn and In nanoparticles, the results of the *LVB* model approached the experimental data at a size larger than 10 nm.

The results of the *SVA* model of  $H_{mb}(r)$  were higher than the experimental results for Ag and In nanoparticles, particularly at a size smaller than ( $r < 15\text{nm}$ ). For In and Sn nanoparticles, the *LVB* and *SVA* models were more consistent with each other at a size of ( $r > 20\text{nm}$ ).

Previously, a physical model was established and predicted that the decrease of size-dependent melting enthalpy,  $H(r)$ , is induced by the increase in *SVA* ratio and lower coordination number of surface atoms [26].

Melting enthalpy changes when nanoparticle size decreases. This trend is due to two reasons; firstly, the surface fraction of atoms in nanoparticles increases with decreasing size and secondly, surface atoms have a different bonding environment than the interior atoms within the material bulk. Moreover, the elastic properties of atoms at the surface differ from those of the bulk, because the phonon confinement affects elasticity and vibration behavior of nanoparticles [29, 31, 39, 40].

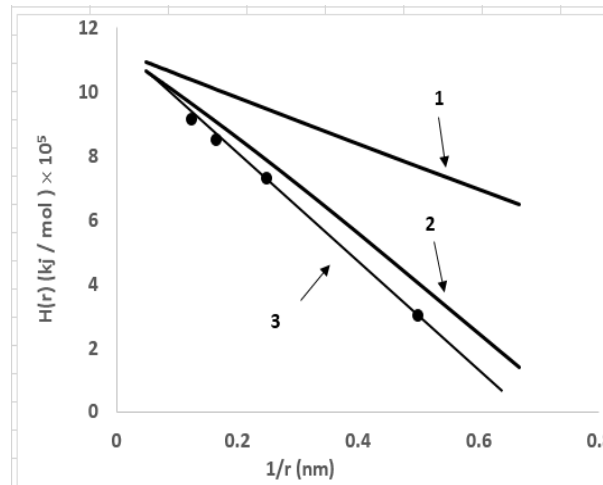


FIG. 3.  $H(r)$  function of Ag nanoparticle size, where number (1) represents the *SVA* model predication of Eq. (17), (2) represents the *LVB* model predication of Eq. (7), (3) is the modified predication of Eq. (7) and the solid spheres ( $\bullet$ ) represent the experimental data obtained from the Ref [21].

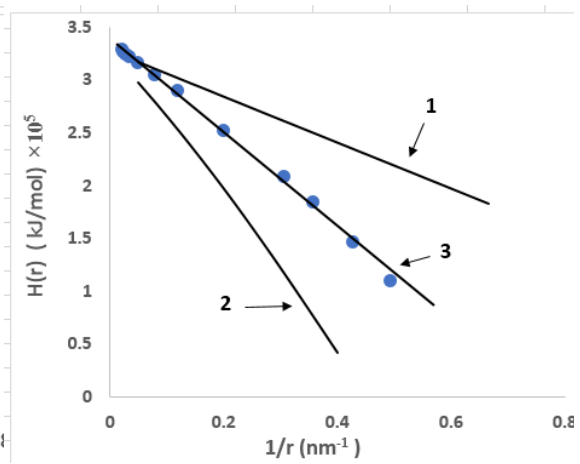


FIG. 4.  $H(r)$  function of In nanoparticle size, where number (1) represents the *SVA* model predication of Eq. (17), (2) represents the *LVB* model predication of Eq. (7), (3) is the modified predication of Eq. (7) and the solid spheres ( $\bullet$ ) represent the experimental data obtained from Ref. [24].

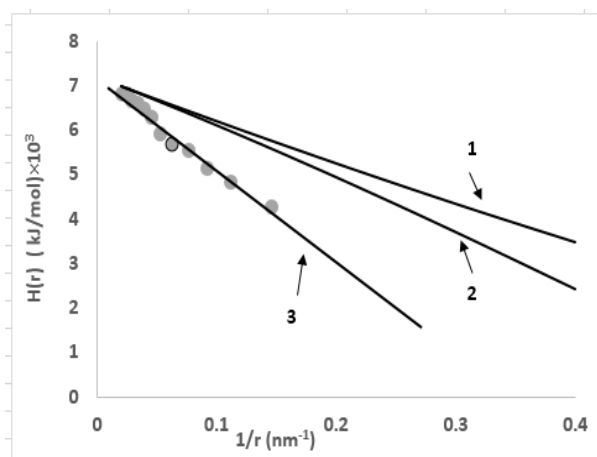


FIG. 5.  $H(r)$  function of Sn nanoparticle size, where number (1) represents the *SVA* model predication of Eq. (17), (2) represents the *LVB* model predication of Eq. (7), (3) is the modified predication of Eq. (7) and the solid spheres (●) represent the experimental data obtained from Ref. [30].

The surface energies of Ag and Au nanoparticles as function of size are shown in Figs. (6) and (7). These figures show that the *LVB* model is better than the *SVA* model, because the surface energy of the *LVB* model approaches the experimental data, particularly for Au nanoparticles, where  $r > 5\text{nm}$ . However, for Ag nanoparticles, matching starts at sizes higher than 10 nm. These results are the reason for the modified *LVB* model. Furthermore, the results of the *SVA* model for Au and Ag nanoparticles were different from the experimental data at the size of ( $r > 10\text{ nm}$ ).

Moreover, good agreement was observed between the modified *LVB* model and the experimental results at low dimensions in Ag and Au nanoparticle sizes near ( $r = 3\text{nm}$ ).

The surface energy of a substance is related to the bonding strength between its atoms. We observed decreased surface energy with decreasing material size. This result was because the atomic radius increased with increasing coordination number [41, 11].

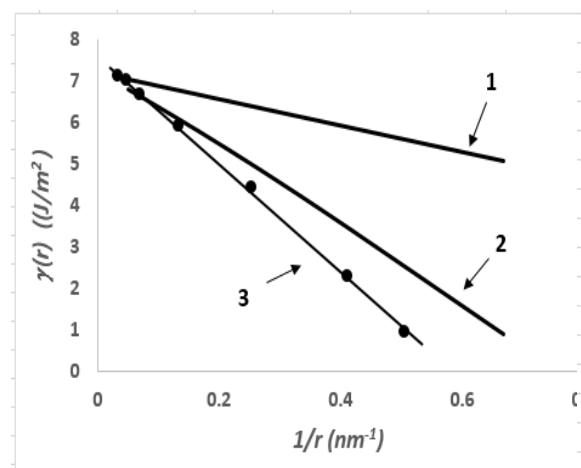


FIG. 6.  $\gamma(r)$  function of Ag nanoparticle size, where number (1) represents the *SVA* model predication of Eq. (20), (2) represents the *LVB* model predication of Eq. (12), (3) is the modified predication of Eq. (12) and the solid spheres (●) represent the experimental data obtained from Ref. [15].

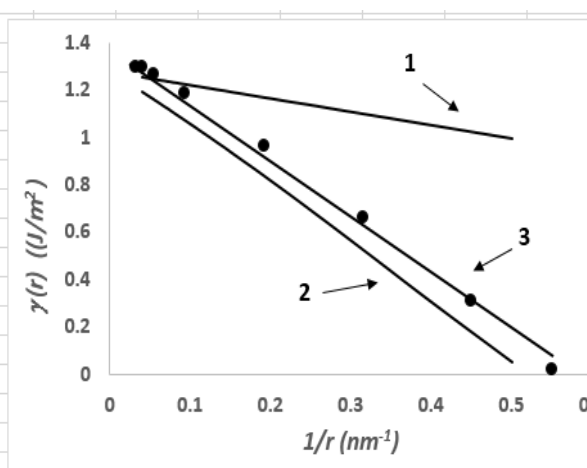


FIG. 7.  $\gamma(r)$  function of Au nanoparticle size, where number (1) represents the *SVA* model predication of Eq. (20), (2) represents the *LVB* model predication of Eq. (11), (3) is the modified predication of Eq. (12) and the solid spheres (●) represent the experimental data obtained from Ref. [37].

Surface atoms take random configuration due to losses in crystalline order [43]. Moreover, surface effects can be neglected for most thermodynamic properties of bulk materials [42].

However, surface effects cannot be ignored for nanoscale metallic materials. Surface effects result from the difference between the surface metallic and interior atoms. Hence, surface atoms will be less stable than inner atoms due to the following: 1) lower coordination number of surface atoms than that of inner atoms and 2) atoms near the surface have fewer bonds than those far from the surface [25, 29].

## Conclusion

In this work, *LVB* and *SVA* models were introduced to study the size-dependent enthalpy, cohesive energy, melting temperature and surface energy of Ag, Au, In and Sn nanoparticles. The relation to calculate thermodynamic parameters for bulk solids is used for nanoscale size successfully after modification. Results showed that the modification of the *LVB* model predication is superior than that of the *SVA* model when comparing the available experimental data, especially with the decrease in the sizes of free-standing nanoparticles. The *LVB* and *SVA* models approach the experimental data at large nanoparticle sizes.

---

## References

- [1] Wang, M., Xue, Y., Cui, Z. and Zhao, M., *J. Mate. Sci.*, 52(2) (2017) 1039.
- [2] Omar, M.S., *J. Mate. Res. Bull.*, 47(11) (2012) 3518.
- [3] Marks, L.D. and Peng, L., *J. Phy. Cond. Matt.*, 28(5) (2016) 053001.
- [4] Li, Q., Yu, Y., Liu, Y., Liu, C. and Lin, L., *A Molecular Dynamics Study. Materials*, 10 (1) (2017) 38.
- [5] Spinozzi, F., Ceccone, G., Moretti, P., Campanella, G., Ferrero, C., Combet, S., Ojea- Jimenez, I. and Ghigna, P., *A Combined SAXS and SANS Study. Langmuir*, 33(9) (2017) 2248.
- [6] Piloyan, G.O., Bortnikov, N.S. and Boeva, N.M., *J. Mod. Phy.*, 4(07) (2013) 16.
- [7] Jiang, Q. and Yang, C.C., *Current Nanoscience*, 4 (2) (2008) 179.
- [8] Nanda, K.K., *Model. Pramana*, 72(4) (2009) 617.
- [9] Jiang, Q., Li, J.C. and Chi, B.Q., *Chem. Phy. Lett.*, 366 (5) (2002) 551.
- [10] Sun, C.Q., Wang, Y., Tay, B.K., Li, S., Huang, H. and Zhang, Y.B., *J. Phy. Chem.*, 106 (41) (2002) 10701.
- [11] Qi, W.H., Wang, M.P., Zhou, M., Shen, X.Q. and Zhang, X.F., *J. Phy. and Chem. Solids*, 67(4) (2006) 851.
- [12] Qi, W.H., Huang, B.Y., Wang, M.P., Li, Z. and Yu, Z.M., *J. Phy. Lett.*, 370 (5) (2007) 494.
- [13] Galanakis, I., Papanikolaou, N. and Dederichs, P.H., *Surface Science*, 511(1) (2002) 12.
- [14] Van Beurden, P. and Kramer, G.J., *Phy. Rev.*, 63(16) (2001) 165106.
- [15] Ouyang, G., Tan, X. and Yang, G., *J. Phy. Rev. B*, 74 (19) (2006) 195408.
- [16] Qi, W.H., Wang, M.P., Li, Z. and Hu, W.Y., *Sol. Stat. Phenomena*, 121 (2007) 1181.
- [17] Diwan, B.D. and Kumar, S.N., *Int. J. Mod. Phy.: Conference Series*, 22 (2013) 525.
- [18] Farrell, H.H., *J. Vac. Scie. and Tech.*, 26 (4) (2008) 1534.
- [19] Lu, H.M. and Jiang, Q., *J. Phy. Chem. B*, 108 (18) (2004) 5617.
- [20] Qi, W.H., *Physica B: Cond. Matt.*, 368 (1) (2005) 46.
- [21] Kumar, R., Sharma, G. and Kumar, M., *J. Thermodynamics*, 213 (2013) 4.
- [22] Omar, M.S., *Int. J. Thermophys.*, 37(11) (2016) 1.
- [23] Sun, C.Q., Bai, H.L., Li, S., Tay, B.K., Li, C., Chen, T.P. and Jiang, E.Y., *J. Phys. Chem.*, 108 (7) (2004) 2162.

- [24] Liang, L.H., Zhao, M. and Jiang, Q., *J. Mat. Sci. Lett.*, 21(23) (2002) 1843.
- [25] Omar, M.S., *J. Adva. Mate. Res.*, 626 (2013) 976.
- [26] Yang, C.C., Xiao, M.X., Li, W. and Jiang, Q., *J. Sol. Sta. Com.*, 139 (4) (2006) 148.
- [27] Farrell, H.H. and Van Siclen, C.D., *J. Vac. Sci. and Tech.*, 25(4) (2007) 1441.
- [28] Yang, C.C. and Li, S., *J. Phy. Chem.*, 112 (42) (2008) 16400.
- [29] Jiang, Q., Shi, H.X. and Zhao, M., *J. Chem. Phy.*, 111(5) (1999) 2176.
- [30] Zhao, M. and Jiang, Q., *Key Engineering Materials*, 444 (2010) 189.
- [31] Liang, L.H., Yang, G.W. and Li, B., *J. Phy. Chem. B*, 109 (33) (2005) 16081.
- [32] Liang, L.H. and Li, B., *Phy. Rev. B*, 73 (15) (2006) 153303.
- [33] Yanfeng, J. and Yamin, Z., *J. Semiconductors*, 31(1) (2010) 012002.
- [34] Singh, M. and Singh, M., *J. Phys.*, 84 (4) (2015) 609.
- [35] Shi, F.G., *J. Mat. Res.*, 9(5) (1994) 1307.
- [36] Vanithakumari, S.C. and Nanda, K.K., *J. Phys. Chem.*, 110 (2) (2006) 1033.
- [37] Jiang, Q. and Lu, H.M., *Surface Sci. Reports*, 63 (10) (2008) 427.
- [38] Buffat, Ph. and Borel, J.P., *Phys. Rev. A*, 6 (1976) 2287.
- [39] Zhang, Z., Lü, X.X. and Jiang, Q., *Phy. Cond. Mat.*, 270 (3) (1999) 249.
- [40] Karasevskii, A.I. and Lubashenko, V.V., arXiv preprint arXiv, (2009) 0902.
- [41] Holec, D., Dumitraschkewitz, P., Fischer, F.D. and Vollath, D., arXiv preprint arXiv, (2014) 1412.7195.
- [42] Ouyang, G., Zhu, W.G., Sun, C.Q., Zhu, Z.M. and Liao, S.Z., *J. Phy. Chem.*, 12 (7), (2010) 1543.
- [43] Regel, A.R. and Glazov, V.M., *J. Semiconductors*, 29 (1995) 405.